Supplementary Material for

Targeting a neoantigen derived from a common *TP53* mutation

Emily Han-Chung Hsiue, Katharine M. Wright, Jacqueline Douglass, Michael S. Hwang, Brian J. Mog, Alexander H. Pearlman, Suman Paul, Sarah R. DiNapoli, Maximilian F. Konig, Qing Wang, Annika Schaefer, Michelle S. Miller, Andrew D. Skora, P. Aitana Azurmendi, Michael B. Murphy, Qiang Liu, Evangeline Watson, Yana Li, Drew M. Pardoll, Chetan Bettegowda, Nickolas Papadopoulos, Kenneth W. Kinzler, Bert Vogelstein*, Sandra B. Gabelli*, Shibin Zhou*

*Corresponding author. Email: vogelbe@jhmi.edu (B.V.); gabelli@jhmi.edu (S.B.G.); sbzhou@jhmi.edu (S.Z.)

Published 1 March 2021 as *Science* First Release
DOI: 10.1126/science.abc8697

This PDF file includes:

Other Supplementary Material for this manuscript includes the following:
(available at science.sciencemag.org/content/science.abc8697/DC1)

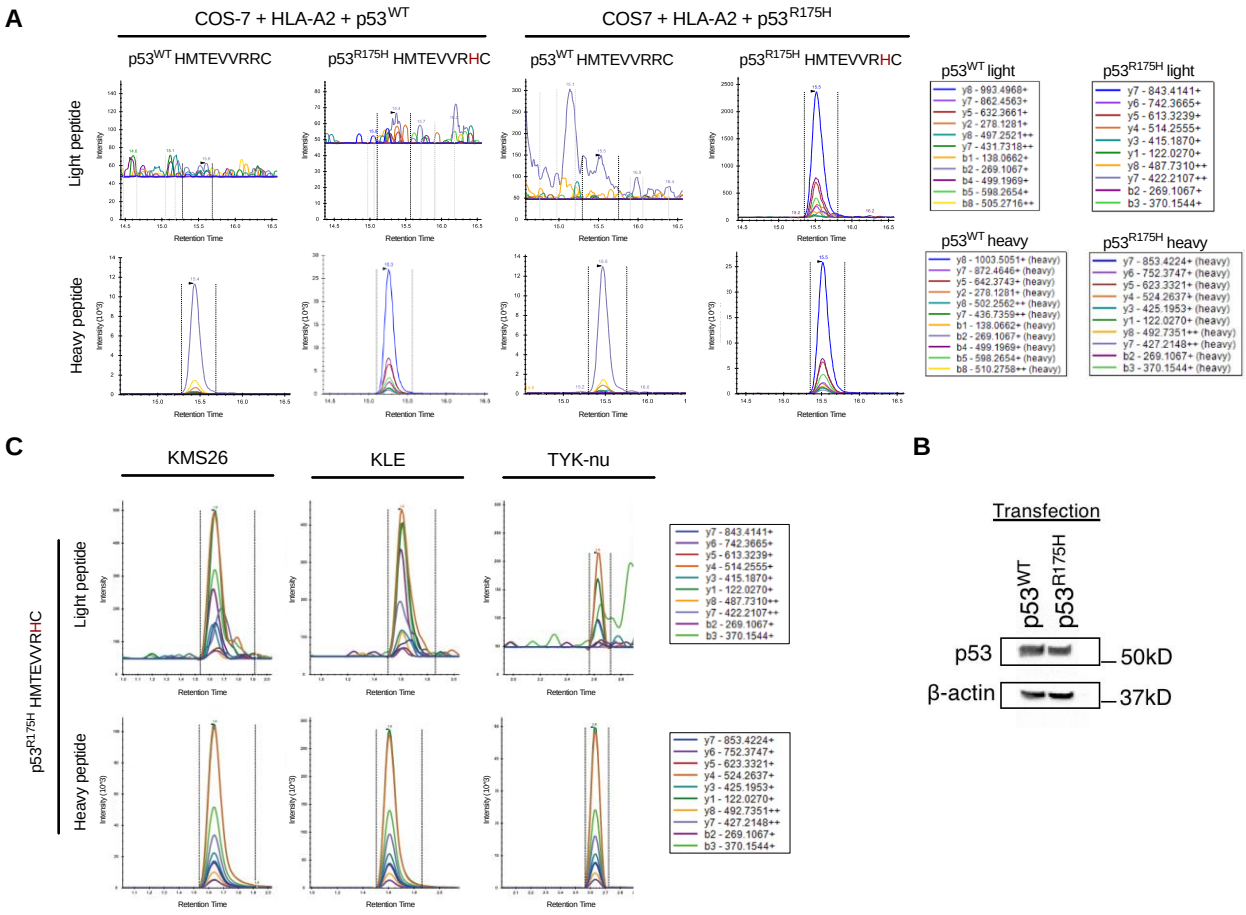

Fig. S1. Detection and quantification of p53^{R175H} peptide in cells. (A) COS-7 cells transfected with constructs expressing HLA-A*02:01 and p53^{WT} or p53^{R175H} were analyzed for the presentation of the p53^{WT} HMTEVVRRC or the p53^{R175H} HMTEVVRHC peptide. Isotope-labeled peptides were spiked into the assay and served as standards for absolute copy number quantification. Multiple ions (indicated by different colors) fragmented from the target peptide in each sample were measured by mass spectrometry as different SRM transitions, and their m/Z values are listed in the figure. (B) Expression of p53 protein in COS-7 cells transfected with plasmids expressing either full-length p53^{WT} or p53^{R175H} was assessed by Western blotting with anti-p53 antibody (clone DO-1). (C) Cell lines with endogenous HLA-A*02:01 and p53^{R175H} expression were analyzed for the presentation of p53^{R175H} peptide as described in (A).

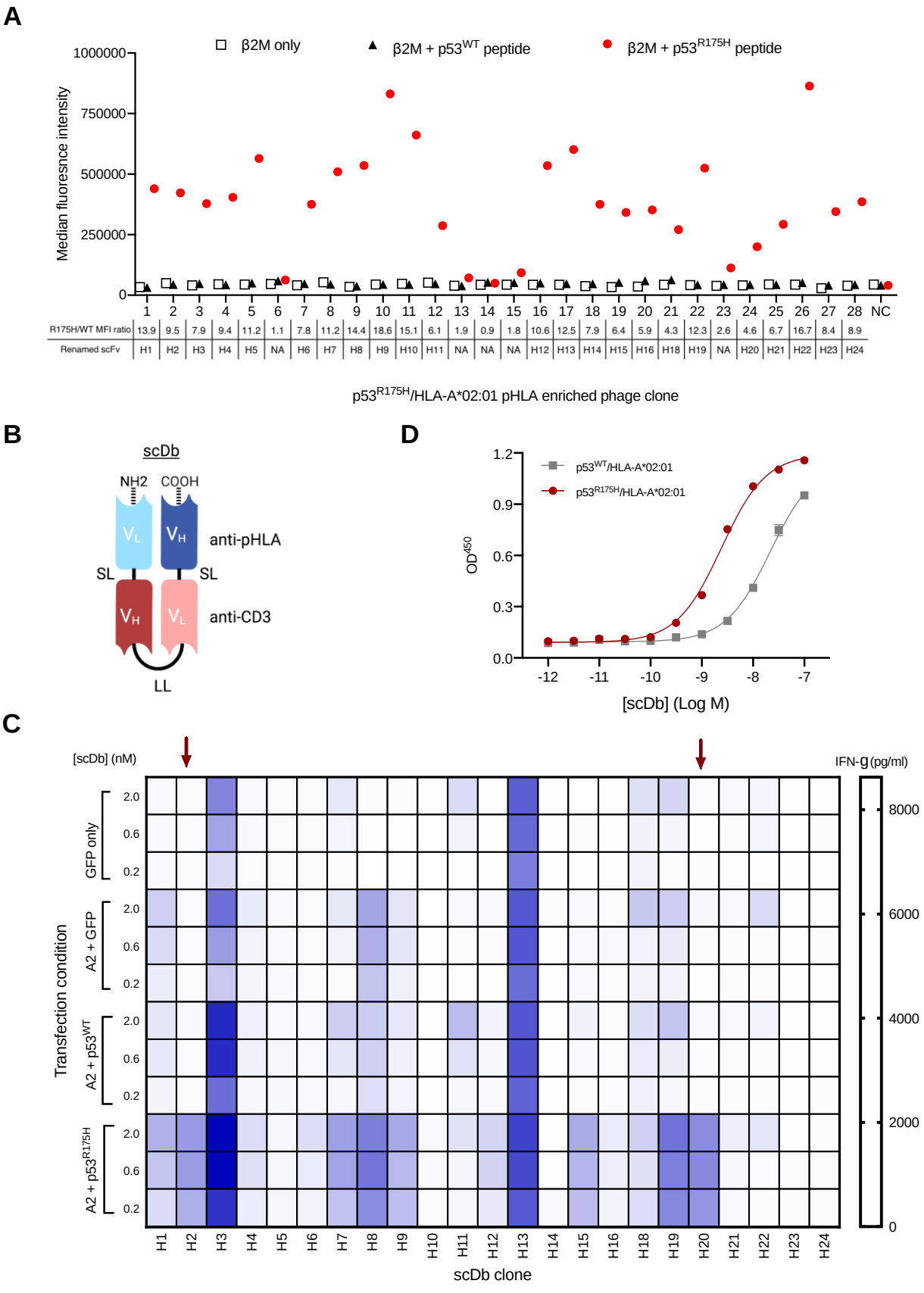
A
β2M only
β2M + p53WT peptide
β2M + p53R175H peptide
Median fluoresnce intensity
1000000
750000
500000
250000
0
1 2 3 4 5 6 7 8 9 10 11 12 13 14 15 16 17 18 19 20 21 22 23 24 25 26 27 28 NC
R175H/WT MFI ratio 13.9 9.5 7.9 9.4 11.2 1.1 7.8 11.2 14.4 18.6 15.1 6.1 1.9 0.9 1.8 10.6 12.5 7.9 6.4 5.9 4.3 12.3 2.6 4.6 6.7 16.7 8.4 8.9
Renamed scFv H1 H2 H3 H4 H5 NA H6 H7 H8 H9 H10 H11 NA NA NA H12 H13 H14 H15 H16 H18 H19 NA H20 H21 H22 H23 H24
p53R175H/HLA-A*02:01 pHLA enriched phage clone
B
scDb
NH2
COOH
VL
VH
anti-pHLA
SL
SL
VH
VL
anti-CD3
LL
D
1.2
0.9
0.6
0.3
0.0
OD450
p53WT/HLA-A*02:01
p53R175H/HLA-A*02:01
-12 -11 -10 -9 -8 -7
[scDb] (Log M)
C
[scDb] (nM)
IFN-g (pg/ml)
8000
6000
4000
2000
0
Transfection condition
GFP only
A2 + GFP
A2 + p53WT
A2 + p53R175H
2.0
0.6
0.2
H1 H2 H3 H4 H5 H6 H7 H8 H9 H10 H11 H12 H13 H14 H15 H16 H18 H19 H20 H21 H22 H23 H24
scDb clone

Fig. S2. Selection of $p53^{R175H}$/HLA-A*02:01 reactive antibodies and their conversion into T cell-retargeting scDb. (A) Flow cytometric screening of phage clones enriched by panning. After 5 rounds of panning, phage clones from the enriched phage pool were isolated by limiting dilution and grown in deep 96-well plates. Supernatants containing individual phage clones were used to assess binding to T2 cells loaded with β2 microglobulin (β2M) only, β2M plus $p53^{WT}$ peptide (HMTEVVRRC), or β2M plus $p53^{R175H}$ peptide (HMTEVVRHC) via flow cytometry. The median fluorescence intensity (MFI) ratio was defined as MFI ($p53^{R175}$ peptide)/MFI ($p53^{WT}$ peptide). NC, no phage control. (B) Schematic representation of the structure of the T cell-engaging bispecific single-chain diabody (scDb) used in our experiments. V_L, variable light domain; V_H, variable heavy domain; pHLA, peptide-HLA complex; SL, short linker; LL, long linker. (C) Screening of scDb clones via IFN-γ stimulation by p53-expressing cells. scDbs generated by linking each anti-$p53^{R175H}$/HLA-A*02:01 pHLA scFv clone with an anti-CD3 scFv (UCHT1) were co-incubated with T cells and COS-7 cells transfected with GFP alone, HLA-A*02:01 + GFP, HLA-A*02:01 + $p53^{WT}$, or HLA-A*02:01 + $p53^{R175H}$ plasmids at an effector:target (E:T) ratio of 1:1. After a 20-hour coincubation, the supernatant was harvested for IFN-γ detection by ELISA. Arrows indicate clones H2 and H20. A2, HLA-A*02:01. (D) Characterization of H20-scDb. H20-scDb was incubated with biotinylated $p53^{WT}$/HLA-A*02:01 (gray) pHLA and $p53^{R175H}$/HLA-A*02:01 (red) monomers coated on streptavidin microplates at the specified concentrations, then binding detected with protein L and anti-protein L HRP. Data indicate mean ± SD of three technical replicates.

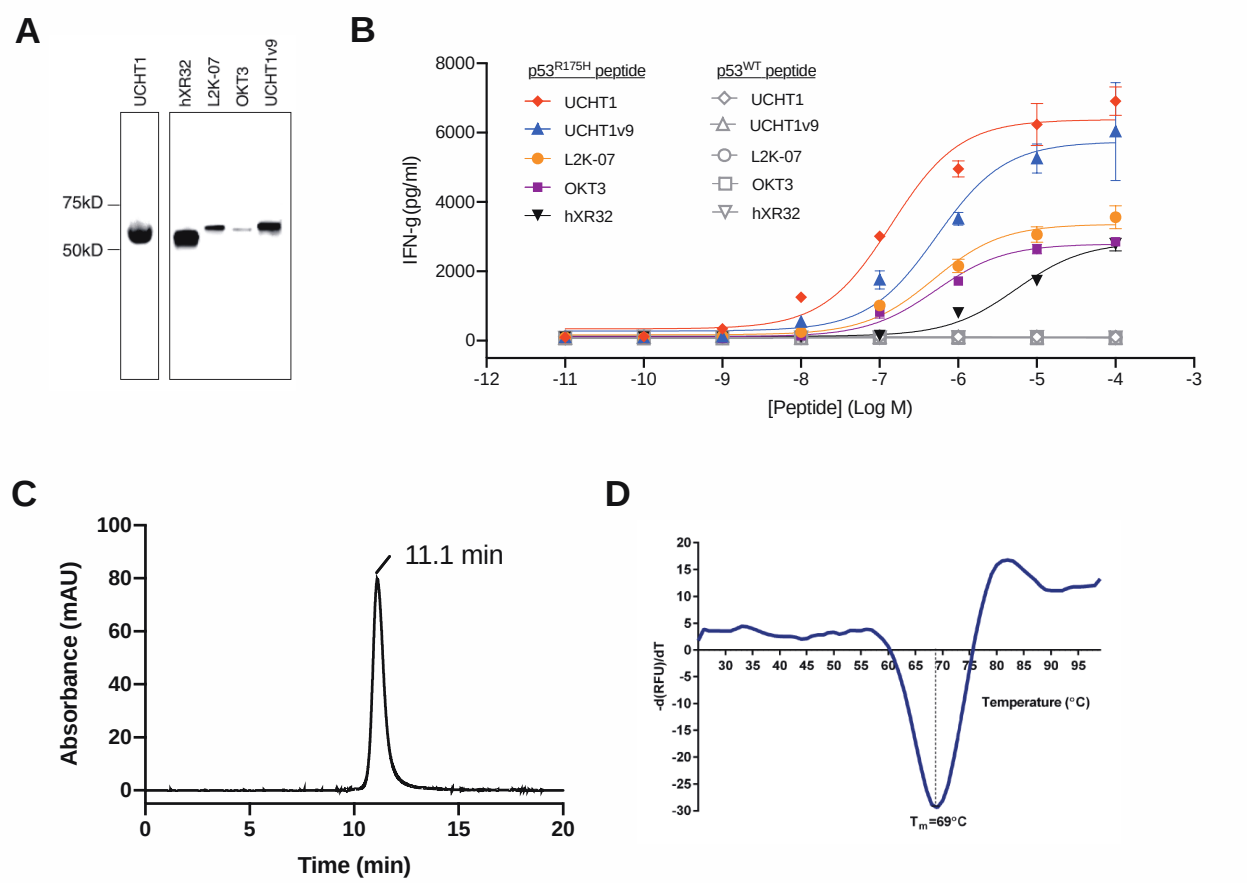

Fig. S3. Characteristics of scDbs generated by linking H2-scFv with anti-CD3ε scFvs. (A) Expression of scDbs composed of linking H2-scFv with different anti-CD3ε scFvs was assessed by anti-6x-His tag Western blotting. (B) The scDbs were co-incubated with T cells and T2 cells pulsed with titrated concentrations of $p53^{WT}$ or $p53^{R175H}$ peptide at an E:T ratio of 2:1. IFN-γ release was measured by ELISA. Data indicate mean ± SD of three technical replicates. (C) Analytical chromatogram of the purified H2-UCHT1-scDb (H2-scDb) showing absorbance at 280 nm. The retention time of the H2-scDb was marked above the peak. (D) DSF analysis of the negative derivative or relative fluorescence unit (RFU) vs. temperature of the H2-scDb. The melting temperature T_m at 69 °C corresponds to the peak/maximum of the first derivative of the curve and the notion of one transition state.

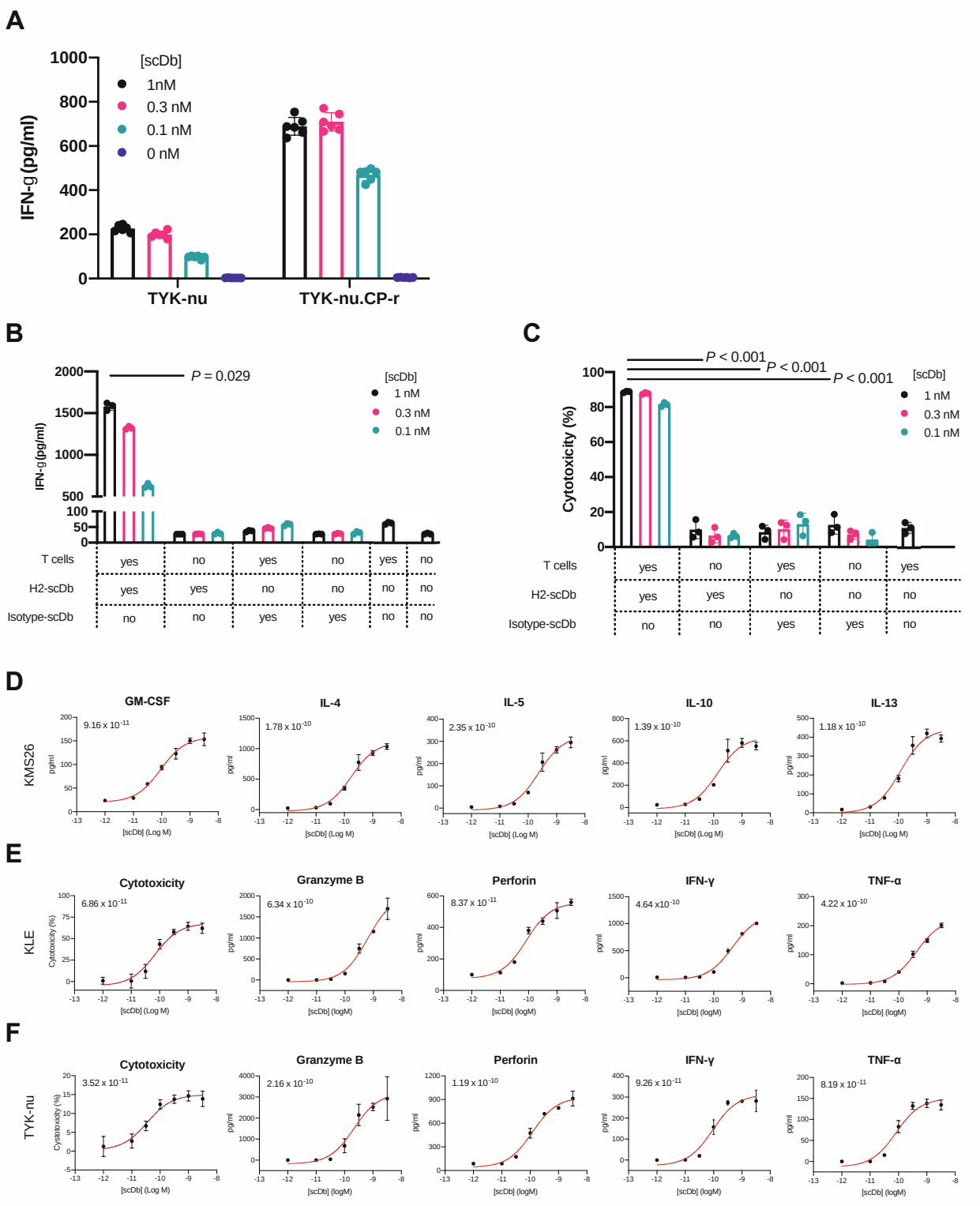

Fig. S4. Reactivity of H2-scDb against p53^{R175H}/HLA-A*02:01-expressing tumor cells. (A) TYK-nu and its cisplatin-resistant subline TYK-nu.CP-r (*77*) were cultured with H2-scDb and T

cells at an E:T ratio of 2:1. IFN-γ release was measured by ELISA. Data indicate mean ± SD of six technical replicates and are representative of two independent experiments. (B, C) KMS26 cells were cultured with H2-scDb or an isotype scDb (scFv against an irrelevant pHLA linked with UCHT1 scFv) in the absence or presence of T cells at an E:T ratio of 2:1. IFN-γ release was measured by ELISA (B), and cytotoxicity was assessed by luminescent assay (C). Data indicate mean ± SD of three technical replicates, analyzed by Kruskal-Wallis test with Dunn's multiple comparisons (B) or one-way analysis of variance (ANOVA) with Tukey's multiple comparisons (C). (D-F) T-cell cytotoxicity and cytokine release mediated by H2-scDb in response to (D) KMS26 (cytotoxicity and other effector proteins shown in main text), (E) KLE, and (F) TYK-nu cell line at an E:T ratio of 2:1 was assessed by antibody-based assays. EC_{50} (M) for each analyte is shown in the corresponding graphs. Data indicate mean ± SD of three technical replicates.

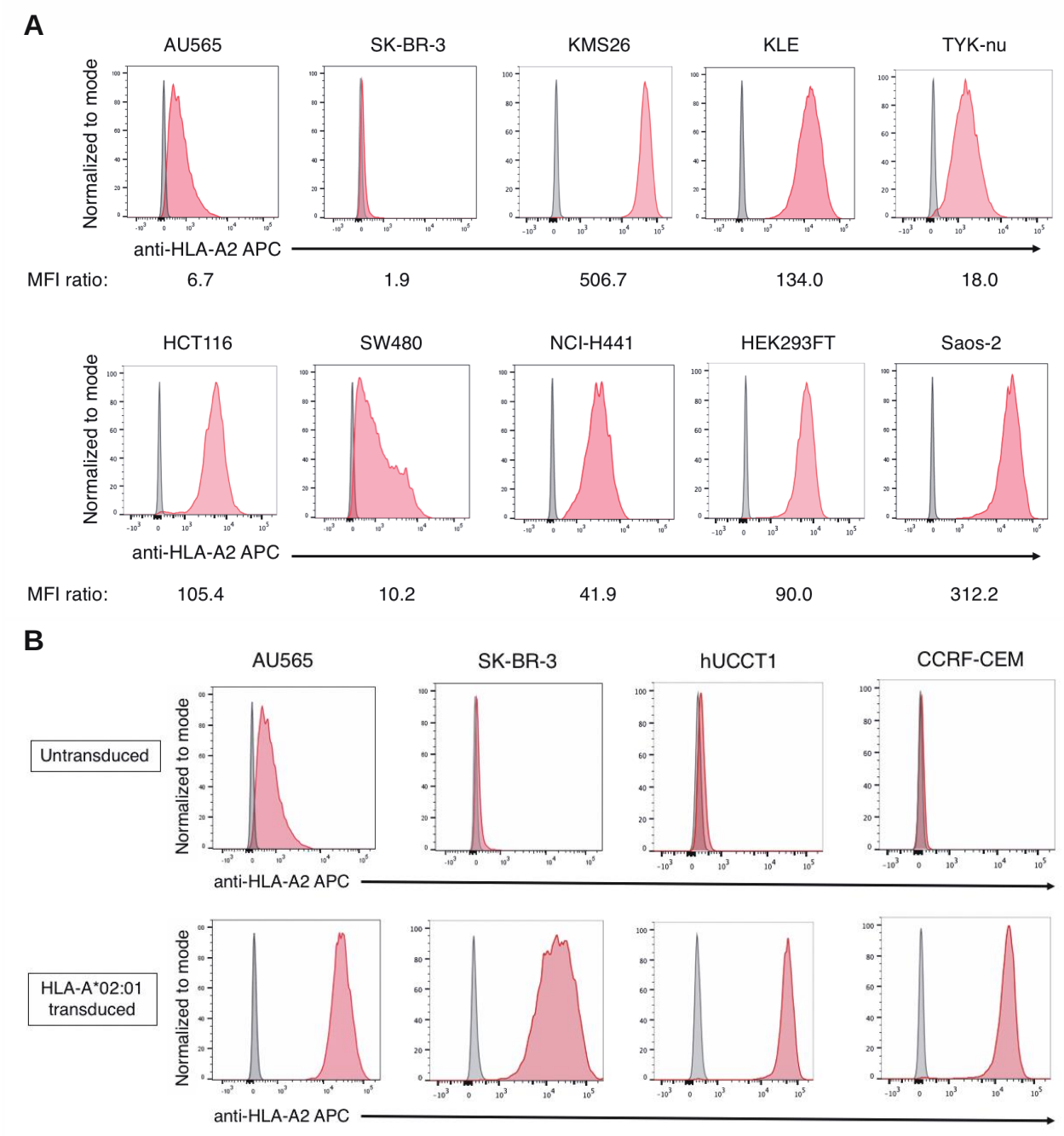

Fig. S5. Flow cytometric evaluation of HLA-A*02 expression. (A) Expression of HLA-A*02 on tumor cell lines was evaluated by flow cytometry. The red histogram represents staining with anti-HLA-A*02 (clone BB7.2, which also recognizes HLA-A*28), and the gray histogram represents staining with an isotype control. The median fluorescence intensity (MFI) ratio is defined as MFI (anti-HLA-A*02)/MFI (isotype control). (B) HLA-A*02:01-expressing

retrovirus was transduced into cell lines that weakly or do not detectably express HLA-A*02:01. Expression of HLA-A*02:01 in the parental as well as transduced and flow-sorted cell lines was evaluated by flow cytometry. The red histogram represents staining with anti-HLA-A*02 (clone BB7.2) and the gray histogram represents staining with an isotype control.

5

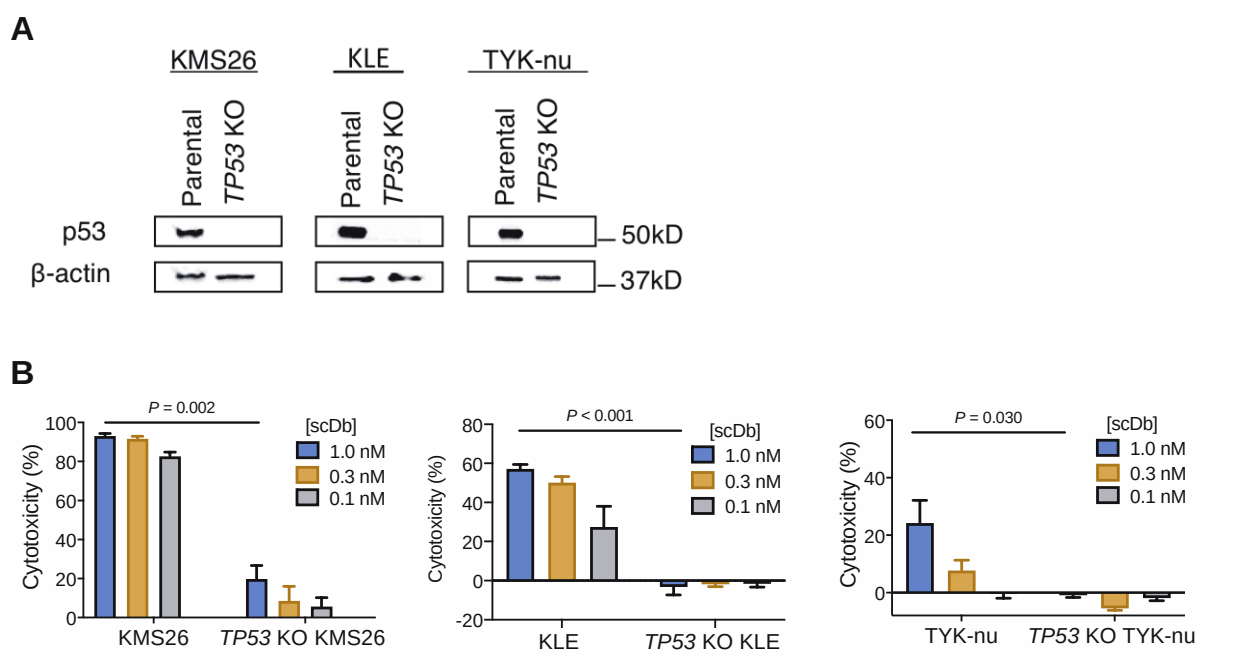

Fig. S6. Determination of H2-scDb specificity using CRISPR-edited isogenic cell lines. (A) Expression of p53 protein in the parental and *TP53* KO clones of KMS26, KLE, and TYK-nu was assessed by Western blot with anti-p53 antibody (clone DO-1). (B) Cytotoxicity mediated by H2-scDb in response to parental tumor cell lines and their *TP53* KO counterparts at an E:T ratio of 2:1 (KMS26, TYK-nu) or 5:1 (KLE) was measured luminescent cytotoxicity assays. Data indicate mean ± SD of three technical replicates and are representative of two independent experiments, analyzed by two-tailed *t*-test.

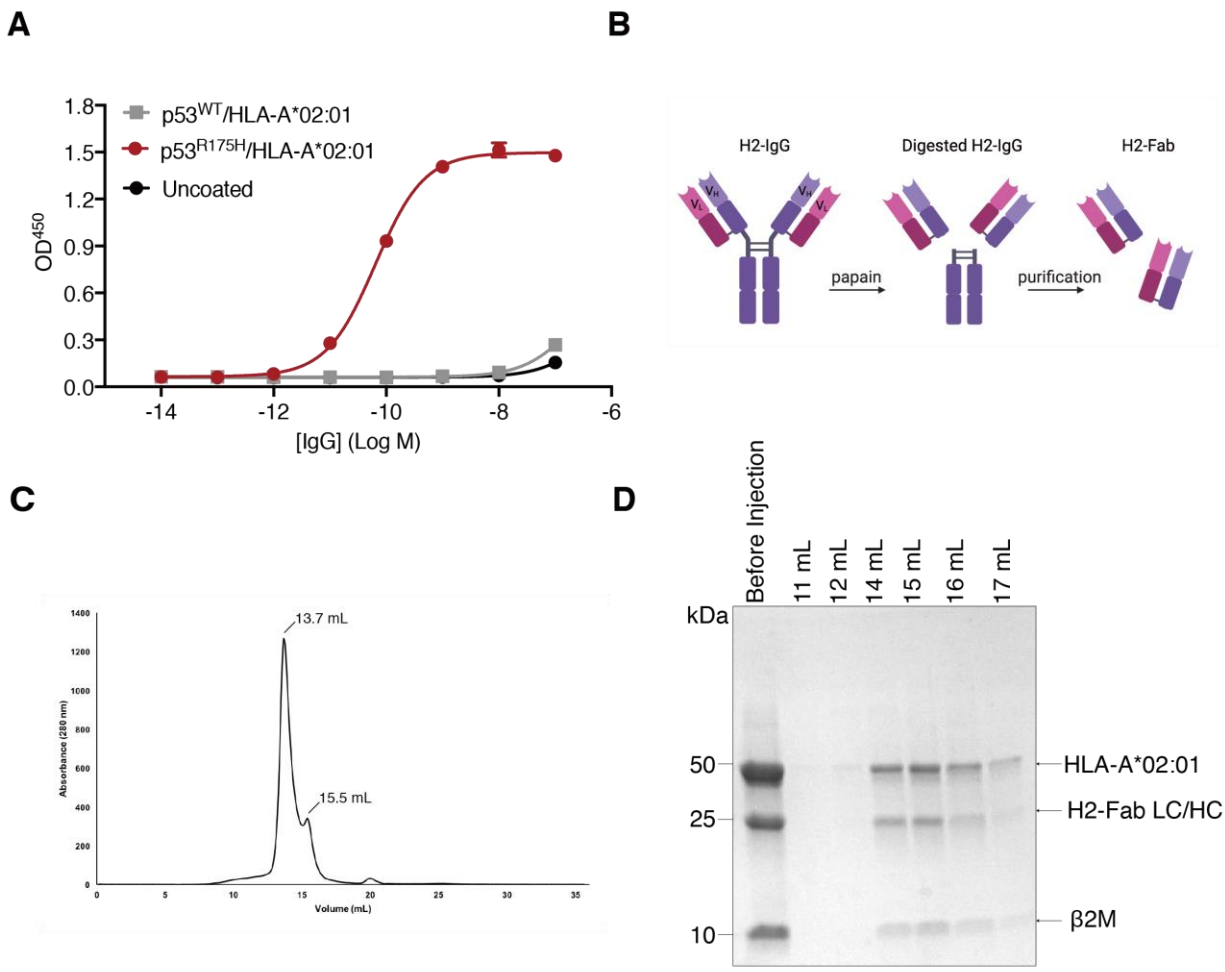

Fig. S7. The H2-Fab–p53^{R175H}/HLA-A*02:01 complex. (A) H2-scFv was converted into full-length IgG (H2-IgG) and incubated with biotinylated p53^{R175H}/HLA-A*02:01 (red) and p53^{WT}/HLA-A*02:01 (gray) pHLA monomers coated on streptavidin microplates at the specified concentrations followed by detection with anti-human IgG HRP. Data indicate mean ± SD of three technical replicates. (B) Illustration depicting the generation of H2-Fab from H2-IgG. (C) Size-exclusion chromatogram of the pHLA-A*02:01 in complex with the H2-Fab. Protein was monitored by A280 nm with a major peak (~100 kDa). (D) Coomassie-stained gradient SDS-polyacrylamide gel electrophoresis gel of the eluted fractions at 11-17 mL from (C).

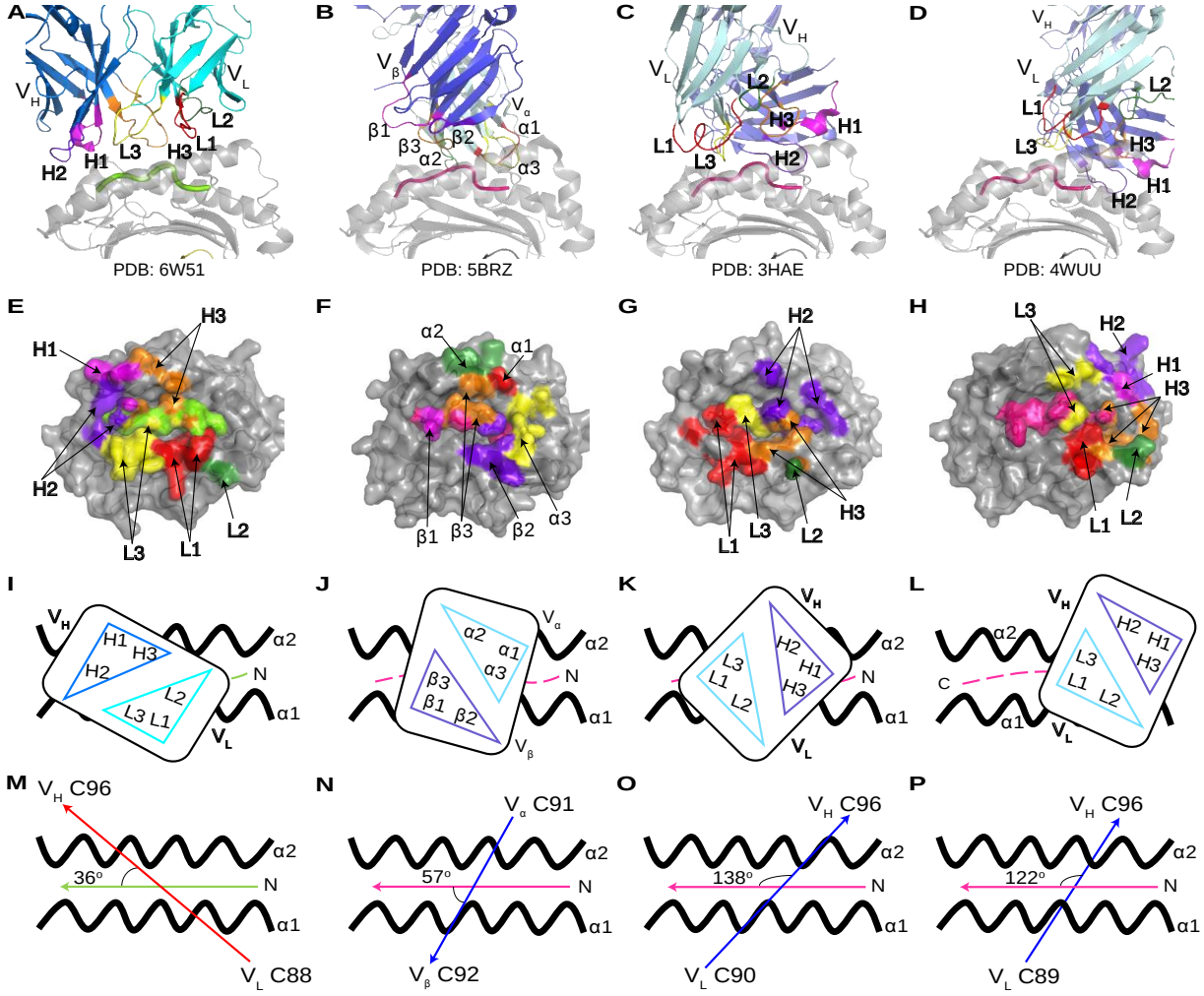

Fig. S8. Comparison of the binding orientations among TCRm–pHLA and TCR–pHLA complexes. (A) Close depiction of binding of the H2-Fab to p53^{R175H}/HLA-A*02:01 with CDRs colored as in Fig. 4. (B) Binding of a TCR to melanoma-associated antigen 3 (MAGE-A3) and HLA-A*01:01 (PDB ID 5BRZ). Same orientation as (A). The MAGE-A3 TCR displays the canonical, diagonal binding motif as that of most known TCR topologies (*47*). (C) Recognition of the 3M4E4 Fab for the NY-ESO-1$_{157-165}$/HLA-A*02:01complex (PDB ID 3HAE) (*46*). Same orientation as (A). (D) Binding of the ESK1 Fab to Wilms tumor 1 peptide and HLA-A*02:01 (PDB ID 4WUU) (*40*). Same orientation as (A). (E, F, G, and H) Bird's-eye view of surface representation of the HLA-A*02:01/*01:01 colored in gray with the contacting residues of H2-

Fab, MAGE-A3 TCR, 3M4E4 Fab, and ESK1 Fab, respectively, colored according to CDRs. (I, J, K, and L) Schematic representation of E, F, G, and H, respectively. H2-Fab–p53^{R175H}/HLA-A*02:01 shows a different mode of antibody recognition compared with other Fab/TCR–pHLA complexes. (M, N, O, and P) Schematic representation of Fab/TCR docking angle for I, J, K, and L, respectively. The docking angle was calculated from the web server TCR3d, which was based on the C^{alpha} of Cys88 (or equivalent) of the disulfide bond of the V_L/α domain and the C^{alpha} of Cys96 (or equivalent) of the disulfide bond of the V_H/β domain of each antibody and TCR. The arrowed lines indicate the direction of each vector. The docking angle was calculated using the web server TCR3d.

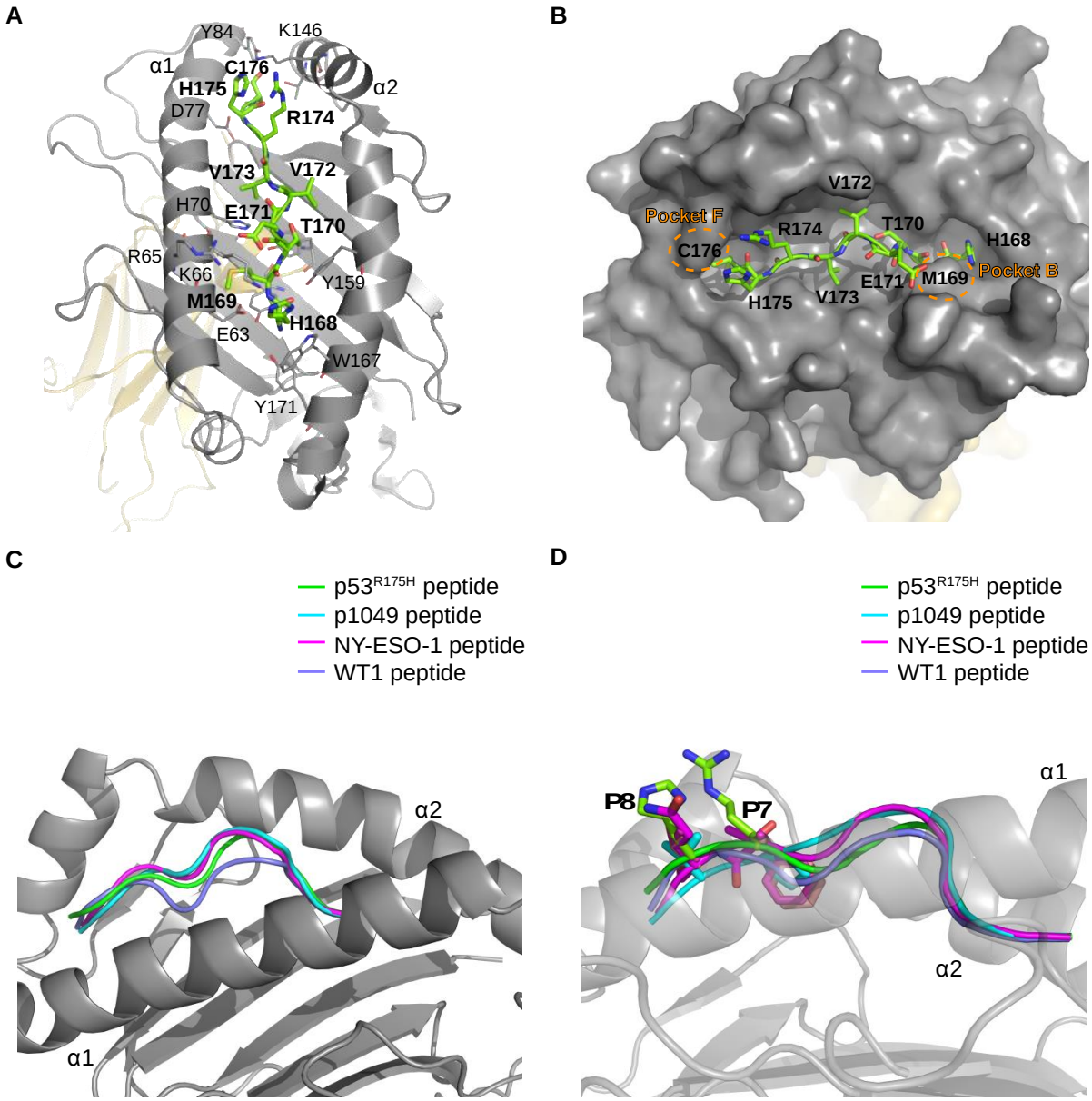

Fig. S9. The neoantigen p53^{R175H} binds to HLA-A*02:01 in a canonical fashion. (A) Bird's-eye view of the p53^{R175H} peptide interactions with HLA-A*02:01. The peptide (green) and the side chains (gray) of interacting residues of HLA-A*02:01 are represented as sticks. Hydrogen bonds are shown as dashed lines. The N-terminal His168 is anchored by three tyrosine residues of HLA-A*02:01, one at the base of the cleft (Tyr7, not shown) and two on α2 (Tyr159, 171), while its side chain is within hydrogen bonding distance of Lys66 (α1) and Thr163 (α2, not

shown). Glu63 of HLA-A*02:01 α1 forms a hydrogen bond with the backbone amino of Met169, an anchor residue of $p53^{R175H}$ that is situated within the hydrophobic B pocket of the HLA. The main chain of Thr170 is stabilized by a hydrogen bond to Tyr99 (not shown), located at the base of the cleft while the side chain of Glu171 forms a salt-bridge with the side chain of Arg65. Positions 5-8 (Val172, Val173, Arg174, His175) of the $p53^{R175H}$ peptide are stabilized by multiple hydrophobic and aliphatic residues with no direct hydrogen bonding contacts to the HLA-A*02:01. Towards the C-terminus of the peptide, the carboxyl group of Cys176, another anchor residue that lies within the F pocket, is secured by Tyr84 (α1) and Lys146 (α2), while the side chain sulfhydryl is near Thr143 on α2. (B) Surface representation of the HLA-A*02:01 (gray) with the $p53^{R175H}$ peptide shown in green as sticks. Anchor pockets B and F are circled in orange. (C) Structural alignment of the following HLA-A*02:01-bound peptides in the binding pocket: green (this work, PDB ID 6W51), cyan (p1049, PDB ID 2JCC (*78*)), magenta (NY-ESO-1, PDB ID 3HAE (*46*)), and light purple (WT1, PDB ID 4WUU (*40*)). (D) Zoomed in view of (B) with helix α1 transparent and residues at positions 7 (P7) and 8 (P8) shown as sticks.

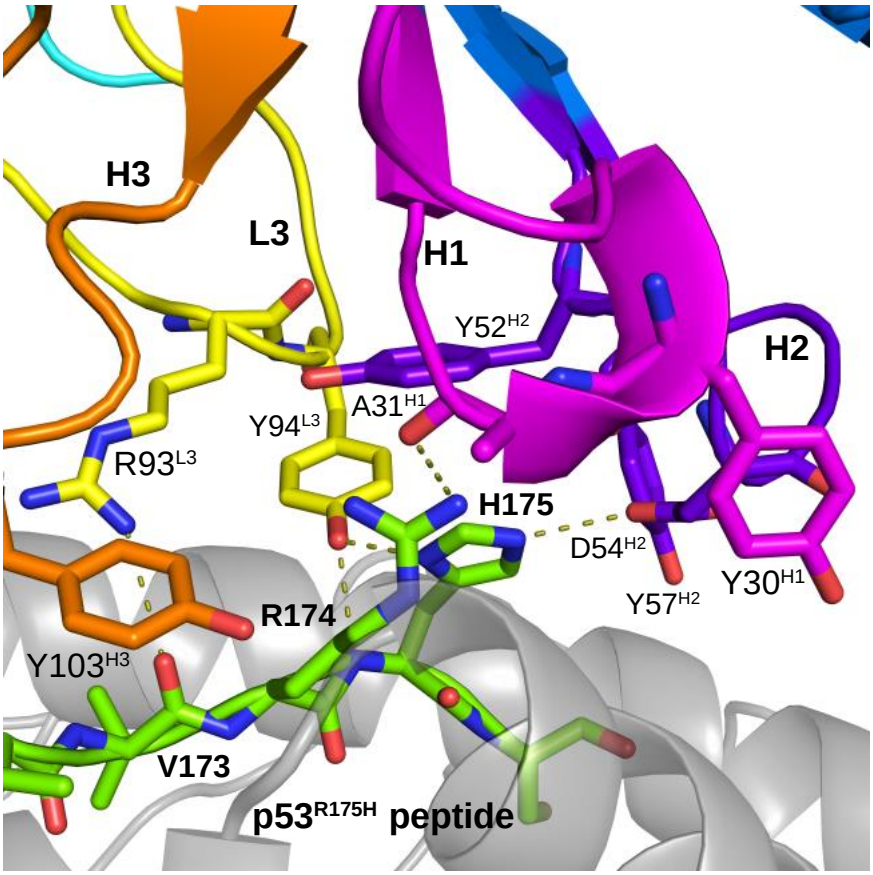

Fig. S10. Hydrogen bonding pattern of the H2-Fab cage-like configuration. The imidazole ring of His175 was at the center from the cage-like structure. The guanidinium group of Arg174 was at hydrogen bonding distance to the backbone carbonyl of Ala31 (CDR-H1). Another $p53^{R175H}$ peptide-antibody direct contact involves the backbone carbonyl of Val173 hydrogen bonding with the side chain of Arg93 (CDR-L3).

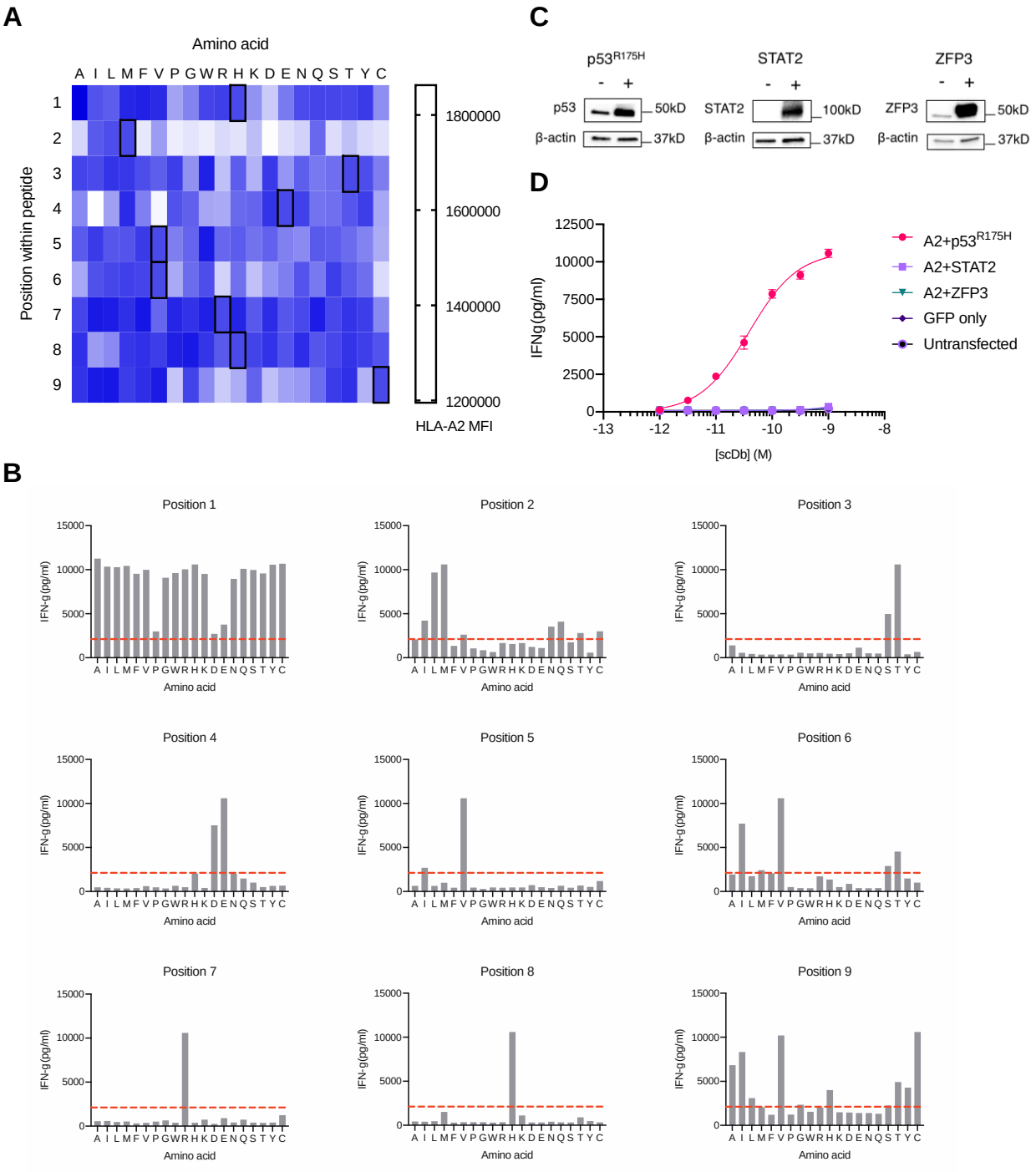

Fig. S11. Assessment of H2-scDb cross-reactivity. (A) A peptide library was generated by systemically substituting the amino acid at each position of the target peptide (HMTEVVRHC) with each of the remaining 19 common amino acids. T2 cells were loaded with each of the variant peptides at 100 μM in the presence of 10 μg/ml β2M and anti-HLA-A*02 antibody

(clone BB7.2). HLA-A*02:01 was stabilized by peptide binding and evaluated by flow cytometry (*79*). Black boxes represent the amino acids in the parental peptide. MFI, median fluorescence intensity. (B) T2 cells loaded with variant peptides in the positional scanning library were incubated with 1 nM H2-scDb and T cells at an E:T ratio of 2:1. IFN-γ release was measured by ELISA. Dotted lines represent 20% of parental peptide IFN-γ value. The binding motif established by the 20% reactivity cutoff, expressed in PROSITE pattern, was x-[ILMVNQTC]-[ST]-[DE]-[IV]-[IMVST]-R-H-[AILVGHSTYC]. Data indicate mean of two technical replicates. (C-D) H2-scDb was co-incubated with T cells and COS-7 cells transfected with plasmids expressing HLA-A*02:01 and full-length $p53^{R175H}$, STAT2, or ZFP3 at an E:T ratio of 5:1. (C) Expression of target proteins by COS-7 cells was assessed by Western blot staining. (D) IFN-γ secretion was measured by ELISA. The signals for all of the transfectants except for $p53^{R175H}$ were indistinguishable and are clustered near the x-axis. Data indicate mean ± SD of three technical replicates and are representative of two independent experiments.

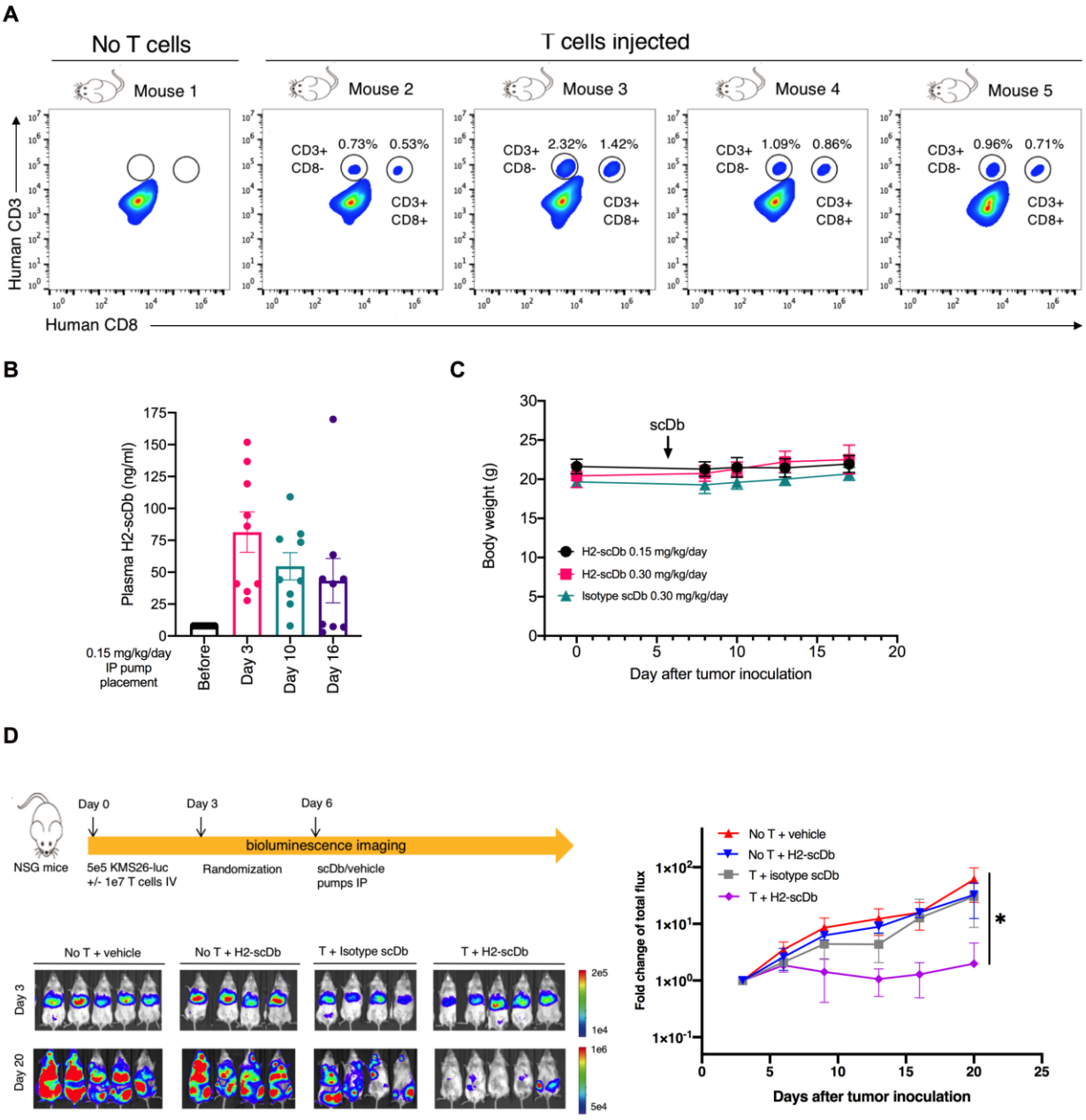

Fig. S12. Assessing T-cell engraftment and effects of H2-scDb therapy in NSG mice. (A) Three days after the injection of KMS26 cells and human T cells, peripheral blood of mice was obtained to assess human T cell engraftment by flow cytometry. Plots shown were gated on live single cells. (B) Plasma of mice was collected 3 days before and 3, 10 and 16 days after the IP implantation of infusion pumps. Plasma concentration of H2-scDb was measured by ELISA. n = 9 mice. Data shown represent mean ± SEM. (C) Serial monitoring of body weight of the mice in

the established KMS26 model presented in Fig. 6B. n = 5 mice per group. Data shown represent mean ± SD. (D) To assess the need for human T-cells in this model, NSG mice were engrafted with 5 x 10^5 KMS26 cells on day 0 with or without 1 x 10^7 human T cells (T) through IV injection, followed by randomization on day 3 and IP placement of infusion pumps on day 6 to deliver H2-scDb or vehicle at the infusion rate of 0.15 mg/kg/day. Tumor growth was monitored by bioluminescence imaging. n = 4 or 5 mice per group. Data shown represent mean ± SD. *No T + vehicle vs. T + H2-scDb, P = 0.008 and 0.049, No T + H2-scDb vs. T + H2-scDb P = 0.011 and 0.054, T + Isotype scDb vs. T + H2-scDb P = 0.021 and 0.078, No T + vehicle vs. No T + H2-scDb P = 0.224 and 0.238 by two-tailed *t*-test at the last time point with and without assuming equal variance, respectively.

Cell line	HLA and p53 status	No. cells (millions) used for analysis	Abundance (femtomole)	Copy no. / cell*
COS-7	Exogenous HLA-A*02:01/p53^{R175H}	375.0	32.43	703.5
COS-7	Exogenous HLA-A*02:01/p53^{WT}	375.0	Not detectable	Not detectable
KMS26	Endogenous HLA-A*02:01/p53^{R175H}	157.0	0.48	2.4
KLE	Endogenous HLA-A*02:01/p53^{R175H}	92.4	0.18	1.5
TYK-nu	Endogenous HLA-A*02:01/p53^{R175H}	168.3	0.28	1.3

Table S1. Quantitative assessment of the p53^{R175H} peptide. The amounts of p53^{R175H} peptide (HMTEVVRHC) present in COS-7 cells transfected with HLA-A*02:01 and p53^{WT} or p53^{R175H}, as well as cell lines that endogenously express HLA-A*02:01 and p53^{R175H}, were quantified using mass spectrometry (*27*). *Corrected for peptide recovery (all cell lines) and transfection efficiency (COS-7).

scFv	VL	VH
H2	DIQMTQSPSSLSASVGDRVTITCRASQ DVNTAVAWYQQKPGKAPKLLIYSAY FLYSGVPSRFSGSRSGTDFTLTISSLQP EDFATYYCQQYSRYSPVTFGQGTKVE IK	EVQLVESGGGLVQPGGSLRLSCAASG FNVYASGMHWVRQAPGKGLEWVAK IYPDSDYTYYADSVKGRFTISADTSKN TAYLQMNSLRAEDTAVYYCSRDSSFY YVYAMDYWGQGTLVTVSS
H20	DIQMTQSPSSLSASVGDRVTITCRASQ DVNTAVAWYQQKPGKAPKLLIYSASF LYSGVPSRFSGSRSGTDFTLTISSLQPE DFATYYCQQSNAYPITFGQGTKVEIK	EVQLVESGGGLVQPGGSLRLSCAASG FNLNSYYMHWVRQAPGKGLEWVAM IIPGYGYTNYADSVKGRFTISADTSKN TAYLQMNSLRAEDTAVYYCSRSYYM YMDYWGQGTLVTVSS

Table S2. Sequences of the top scFv clones from phage library selection

anti-CD3ε scFv clone	Reported affinity (K_D, nM)	Format in which affinity was measured	References
UCHT1	1.8	Full-length antibody	(*80*)
UCHT1v9	4.7	Full-length bispecific antibody	*(81)*
L2K-07	110	Bispecific T-cell engager (BiTE)	*(82)*
OKT3	2730	Fab	*(83)*
hXR32	21.2	Dual affinity retargeting (DART) protein	*(84)*

Table S3. Reported affinities of the anti-human CD3ε scFvs used in this study.

	$p53^{R175H}$/HLA-A*02:01–Fab H2 (PDB ID 6W51)
Data Collection	
Diffraction source	NSLS-II X17-ID-2
Wavelength (Å)	0.979321
Temperature (K)	100
Detector	Dectris EIGER X 16M
Space group	$P12_11$
a, b, c (Å)	113.3, 123.7, 136.9
α, β, γ (°)	90, 100.4, 90
Resolution range (Å)	30.37–3.53 (3.66-3.53)
Total no. of reflections	104,474 (9,774)
No. of unique reflections	43,734 (4,273)
Completeness (%)	95.3 (89.2)
Redundancy	2.4 (2.3)
$\langle I/\sigma(I)\rangle$	3.6 (1.4)
R_{merge}	0.25 (0.76)
R_{meas}	0.29 (0.89)
R_{pim}	0.18 (0.58)
$CC_{1/2}$	0.94 (0.54)
Refinement	
Resolution range (Å)	30.38-3.53 (3.62-3.53)
No. of reflections, working set	41,530
R_{work}/R_{free}	0.20/0.28 (0.30/0.35)
No. of non-H atoms	
MHC (HLA-A*02:01 + β2m)	3,078
$p53^{R175H}$ peptide	75
Fab H2 Heavy Chain	1,667
Fab H2 Light Chain	1,652
Total of non-H atoms	6,472
R.m.s. deviations	
Bonds (Å)	0.009
Angles (°)	1.66
Wilson B-factor ($Å^2$)	62
Average B factors ($Å^2$)	
MHC (HLA-A*02:01 + β2m)	74
$p53^{R175H}$ peptide	56
Fab H2 Heavy Chain	59
Fab H2 Light Chain	63
Total average B factor	63
Ramachandran (%)	
Favorable	95.2
Allowed	3.8
Outlier	1.0

*Values in parentheses are for highest-resolution shell. All atoms refer to non-H atoms.

Table S4. X-ray crystallography data collection and refinement statistics.

	Chains M, N (Å/#C^{alpha})	**Chains S, T (Å/#C^{alpha})**	**Chains Q, R (Å/#C^{alpha})**
Chains O, P	0.32/382	0.36/414	0.42/413
Chains Q, R	0.45/419	0.27/386	0
Chains S, T	0.34/408	0	**–**

Table S5. Pairwise rmsd of the four H2-Fab in the asymmetric unit. The root-mean square deviation (rmsd) and number of C^{alpha} carbons were calculated by PyMOL (v2.2.3, Schrödinger, LLC). For chain reference see PDB ID 6W51.

	H2-Fab	MAGE-A3 TCR	NY-ESO-1 Fab (3M4E4)	ESK-1 Fab
Affinity (K_D)	86 nM	7.1 nM	95 nM	13.2 nM
PDB	6W51	5BRZ	3HAE	4WUU
Angle of rotation (^{o})	36^o	57^o	138^o	122^o
Total bonds	115	114	167	183
Peptide bonds **(bold ≥10)**	4, 5, 6, **7**, **8**	1, 4, 5, 7, 8	1, 2, **4**, **5**, 6, 7, **8,** 9	**1**, 4
Peptide bonds	36 (31%)	16 (14%)	89 (53%)	19 (10%)
Bonds from β/H	21	10	47	10
Bonds from α/L	15	6	42	9
HLA bonds	79	98	78	164
Bonds from β/H	31	20	47	130
Bonds from α/L	48	78	31	34
HLA ≥5 bonds **(bold ≥10)**	**61**, **65**, 72, 80, 146, **155**	66, **154**, 155, **157**, **158**, **163**	**65**, 66, **72**, 73	**58**, 62, **63**, 65, **66**, 155, 161, 162, **166**, **167**, **169**, **170**
BSA				
BSA total	1173	1027	1366	1084
BSA β/H pep	253	158	256	72
BSA α/L pep	102	112	260	93
BSA β/H HLA	391	247	523	601
BSA α/L HLA	427	510	327	318

Table S6. Structural comparison of H2-Fab–p53^{R175H}/ HLA-A*02:01 with various TCR and Fab antibody-pHLA. Total bonds were calculated using a 4 Å cutoff which includes both hydrogen bonds and van der Waals interactions as calculated using CONTACTS in the CCP4 suite (*74*). PDB, Protein Data Bank; BSA, buried surface area; α, TCRα chain; β, TCRβ chain; H, V_H domain; L, V_L domain; pep, HLA presented peptide.

UniProt ID	Name	Peptide position	Sequence	HLA-A*02:01 Affinity (nM)	%Rank
NA	$p53^{R175H}$	168-176	HMTEVVRHC	5177.6	9.7
P52630	STAT2	640-648	PLTEIIRHY	32385.4	46.8
Q96RL7	VPS13A	2840-2848	LQSEVIRHY	21897.4	27.6
Q96NJ6	ZFP3	348-356	QNSEIIRHI	31174.4	43.9

Table S7. Putative cross-reactive peptides identified through positional peptide scanning. A binding motif of H2-scDb was determined by positional scanning of the $p53^{R175H}$ HMTEVVRHC peptide. Three peptides that conformed to this motif in the UniProtKB human protein database were identified using ScanProsite (*45*). NetMHCPan4.0 was used to predict the binding affinity and % rank of these peptides to HLA-A*02:01 (*25*). The parental $p53^{R175H}$ target peptide is listed for comparison.

Movie S1. Real-time live-cell analysis of H2-scDb induced T cell cytolysis of cancer cells

Time-lapse imaging visualizing co-incubation of NucLight Green-labeled TYK-nu cells with 1 nM H2-scDb and T cells at an E:T ratio of 5:1. Representative phase contrast and green fluorescence images were taken at 3-hour intervals for a total of 120 hours and merged for each time point.

References and Notes

1. L. B. Alexandrov, S. Nik-Zainal, D. C. Wedge, S. A. Aparicio, S. Behjati, A. V. Biankin, G. R. Bignell, N. Bolli, A. Borg, A. L. Børresen-Dale, S. Boyault, B. Burkhardt, A. P. Butler, C. Caldas, H. R. Davies, C. Desmedt, R. Eils, J. E. Eyfjörd, J. A. Foekens, M. Greaves, F. Hosoda, B. Hutter, T. Ilicic, S. Imbeaud, M. Imielinski, N. Jäger, D. T. Jones, D. Jones, S. Knappskog, M. Kool, S. R. Lakhani, C. López-Otín, S. Martin, N. C. Munshi, H. Nakamura, P. A. Northcott, M. Pajic, E. Papaemmanuil, A. Paradiso, J. V. Pearson, X. S. Puente, K. Raine, M. Ramakrishna, A. L. Richardson, J. Richter, P. Rosenstiel, M. Schlesner, T. N. Schumacher, P. N. Span, J. W. Teague, Y. Totoki, A. N. Tutt, R. Valdés-Mas, M. M. van Buuren, L. van 't Veer, A. Vincent-Salomon, N. Waddell, L. R. Yates, J. Zucman-Rossi, P. A. Futreal, U. McDermott, P. Lichter, M. Meyerson, S. M. Grimmond, R. Siebert, E. Campo, T. Shibata, S. M. Pfister, P. J. Campbell, M. R. Stratton, Australian Pancreatic Cancer Genome Initiative, ICGC Breast Cancer Consortium, ICGC MMML-Seq Consortium, ICGC PedBrain, Signatures of mutational processes in human cancer. *Nature* **500**, 415–421 (2013). doi:10.1038/nature12477 Medline

2. B. Vogelstein, N. Papadopoulos, V. E. Velculescu, S. Zhou, L. A. Diaz Jr., K. W. Kinzler, Cancer genome landscapes. *Science* **339**, 1546–1558 (2013). doi:10.1126/science.1235122 Medline

3. L. A. Garraway, E. S. Lander, Lessons from the cancer genome. *Cell* **153**, 17–37 (2013). doi:10.1016/j.cell.2013.03.002 Medline

4. M. Gerstung, C. Jolly, I. Leshchiner, S. C. Dentro, S. Gonzalez, D. Rosebrock, T. J. Mitchell, Y. Rubanova, P. Anur, K. Yu, M. Tarabichi, A. Deshwar, J. Wintersinger, K. Kleinheinz, I. Vázquez-García, K. Haase, L. Jerman, S. Sengupta, G. Macintyre, S. Malikic, N. Donmez, D. G. Livitz, M. Cmero, J. Demeulemeester, S. Schumacher, Y. Fan, X. Yao, J. Lee, M. Schlesner, P. C. Boutros, D. D. Bowtell, H. Zhu, G. Getz, M. Imielinski, R. Beroukhim, S. C. Sahinalp, Y. Ji, M. Peifer, F. Markowetz, V. Mustonen, K. Yuan, W. Wang, Q. D. Morris, P. T. Spellman, D. C. Wedge, P. Van Loo, S. C. Sahinalp, Y. Ji, M. Peifer, F. Markowetz, V. Mustonen, K. Yuan, W. Wang, Q. D. Morris, P. T. Spellman, D. C. Wedge, P. Van Loo, PCAWG Evolution and Heterogeneity Working Group, PCAWG Consortium, The evolutionary history of 2,658 cancers. *Nature* **578**, 122–128 (2020). doi:10.1038/s41586-019-1907-7 Medline

5. L. Bouaoun, D. Sonkin, M. Ardin, M. Hollstein, G. Byrnes, J. Zavadil, M. Olivier, TP53 Variations in Human Cancers: New Lessons from the IARC TP53 Database and Genomics Data. *Hum. Mutat.* **37**, 865–876 (2016). doi:10.1002/humu.23035 Medline

6. M. Hollstein, D. Sidransky, B. Vogelstein, C. C. Harris, p53 mutations in human cancers. *Science* **253**, 49–53 (1991). doi:10.1126/science.1905840 Medline

7. P. Malekzadeh, A. Pasetto, P. F. Robbins, M. R. Parkhurst, B. C. Paria, L. Jia, J. J. Gartner, V. Hill, Z. Yu, N. P. Restifo, A. Sachs, E. Tran, W. Lo, R. P. Somerville, S. A. Rosenberg, D. C. Deniger, Neoantigen screening identifies broad TP53 mutant immunogenicity in patients with epithelial cancers. *J. Clin. Invest.* **129**, 1109–1114 (2019). doi:10.1172/JCI123791 Medline

8. W. Lo, M. Parkhurst, P. F. Robbins, E. Tran, Y. C. Lu, L. Jia, J. J. Gartner, A. Pasetto, D. Deniger, P. Malekzadeh, T. E. Shelton, T. Prickett, S. Ray, S. Kivitz, B. C. Paria, I. Kriley, D. S. Schrump, S. A. Rosenberg, Immunologic recognition of a shared p53 mutated neoantigen in a patient with metastatic colorectal cancer. *Cancer Immunol. Res.* **7**, 534–543 (2019). doi:10.1158/2326-6066.CIR-18-0686 Medline

9. R. L. Grossman, A. P. Heath, V. Ferretti, H. E. Varmus, D. R. Lowy, W. A. Kibbe, L. M. Staudt, Toward a shared vision for cancer genomic data. *N. Engl. J. Med.* **375**, 1109–1112 (2016). doi:10.1056/NEJMp1607591 Medline

10. F. F. González-Galarza, L. Y. Takeshita, E. J. Santos, F. Kempson, M. H. Maia, A. L. da Silva, A. L. Teles e Silva, G. S. Ghattaoraya, A. Alfirevic, A. R. Jones, D. Middleton, Allele frequency net 2015 update: New features for HLA epitopes, KIR and disease and HLA adverse drug reaction associations. *Nucleic Acids Res.* **43** (D1), D784–D788 (2015). doi:10.1093/nar/gku1166 Medline

11. T. Dao, S. Yan, N. Veomett, D. Pankov, L. Zhou, T. Korontsvit, A. Scott, J. Whitten, P. Maslak, E. Casey, T. Tan, H. Liu, V. Zakhaleva, M. Curcio, E. Doubrovina, R. J. O'Reilly, C. Liu, D. A. Scheinberg, Targeting the intracellular WT1 oncogene product with a therapeutic human antibody. *Sci. Transl. Med.* **5**, 176ra33 (2013). doi:10.1126/scitranslmed.3005661 Medline

12. A. Y. Chang, T. Dao, R. S. Gejman, C. A. Jarvis, A. Scott, L. Dubrovsky, M. D. Mathias, T. Korontsvit, V. Zakhaleva, M. Curcio, R. C. Hendrickson, C. Liu, D. A. Scheinberg, A therapeutic T cell receptor mimic antibody targets tumor-associated PRAME peptide/HLA-I antigens. *J. Clin. Invest.* **127**, 2705–2718 (2017). doi:10.1172/JCI92335 Medline

13. D. Li, C. Bentley, A. Anderson, S. Wiblin, K. L. S. Cleary, S. Koustoulidou, T. Hassanali, J. Yates, J. Greig, M. O. Nordkamp, I. Trenevska, N. Ternette, B. M. Kessler, B. Cornelissen, M. S. Cragg, A. H. Banham, Development of a T-cell receptor mimic antibody against wild-type p53 for cancer immunotherapy. *Cancer Res.* **77**, 2699–2711 (2017). doi:10.1158/0008-5472.CAN-16-3247 Medline

14. L. Low, A. Goh, J. Koh, S. Lim, C.-I. Wang, Targeting mutant p53-expressing tumours with a T cell receptor-like antibody specific for a wild-type antigen. *Nat. Commun.* **10**, 5382 (2019). doi:10.1038/s41467-019-13305-z Medline

15. T. Dao, D. Pankov, A. Scott, T. Korontsvit, V. Zakhaleva, Y. Xu, J. Xiang, S. Yan, M. D. de Morais Guerreiro, N. Veomett, L. Dubrovsky, M. Curcio, E. Doubrovina, V. Ponomarev, C. Liu, R. J. O'Reilly, D. A. Scheinberg, Therapeutic bispecific T-cell engager antibody targeting the intracellular oncoprotein WT1. *Nat. Biotechnol.* **33**, 1079–1086 (2015). doi:10.1038/nbt.3349 Medline

16. C. A. Klebanoff, S. A. Rosenberg, N. P. Restifo, Prospects for gene-engineered T cell immunotherapy for solid cancers. *Nat. Med.* **22**, 26–36 (2016). doi:10.1038/nm.4015 Medline

17. S. Rafiq, T. J. Purdon, A. F. Daniyan, M. Koneru, T. Dao, C. Liu, D. A. Scheinberg, R. J. Brentjens, Optimized T-cell receptor-mimic chimeric antigen receptor T cells directed toward the intracellular Wilms Tumor 1 antigen. *Leukemia* **31**, 1788–1797 (2017). doi:10.1038/leu.2016.373 Medline

18. S. L. Maude, N. Frey, P. A. Shaw, R. Aplenc, D. M. Barrett, N. J. Bunin, A. Chew, V. E. Gonzalez, Z. Zheng, S. F. Lacey, Y. D. Mahnke, J. J. Melenhorst, S. R. Rheingold, A. Shen, D. T. Teachey, B. L. Levine, C. H. June, D. L. Porter, S. A. Grupp, Chimeric antigen receptor T cells for sustained remissions in leukemia. *N. Engl. J. Med.* **371**, 1507–1517 (2014). doi:10.1056/NEJMoa1407222 Medline

19. J. H. Park, I. Rivière, M. Gonen, X. Wang, B. Sénéchal, K. J. Curran, C. Sauter, Y. Wang, B. Santomasso, E. Mead, M. Roshal, P. Maslak, M. Davila, R. J. Brentjens, M. Sadelain, Long-Term Follow-up of CD19 CAR Therapy in acute lymphoblastic leukemia. *N. Engl. J. Med.* **378**, 449–459 (2018). doi:10.1056/NEJMoa1709919 Medline

20. S. J. Schuster, M. R. Bishop, C. S. Tam, E. K. Waller, P. Borchmann, J. P. McGuirk, U. Jäger, S. Jaglowski, C. Andreadis, J. R. Westin, I. Fleury, V. Bachanova, S. R. Foley, P. J. Ho, S. Mielke, J. M. Magenau, H. Holte, S. Pantano, L. B. Pacaud, R. Awasthi, J. Chu, Ö. Anak, G. Salles, R. T. Maziarz; JULIET Investigators, Tisagenlecleucel in adult relapsed or refractory diffuse large B-cell lymphoma. *N. Engl. J. Med.* **380**, 45–56 (2019). doi:10.1056/NEJMoa1804980 Medline

21. P. F. Robbins, S. H. Kassim, T. L. Tran, J. S. Crystal, R. A. Morgan, S. A. Feldman, J. C. Yang, M. E. Dudley, J. R. Wunderlich, R. M. Sherry, U. S. Kammula, M. S. Hughes, N. P. Restifo, M. Raffeld, C. C. Lee, Y. F. Li, M. El-Gamil, S. A. Rosenberg, A pilot trial using lymphocytes genetically engineered with an NY-ESO-1-reactive T-cell receptor: Long-term follow-up and correlates with response. *Clin. Cancer Res.* **21**, 1019–1027 (2015). doi:10.1158/1078-0432.CCR-14-2708 Medline

22. S. Rafiq, C. S. Hackett, R. J. Brentjens, Engineering strategies to overcome the current roadblocks in CAR T cell therapy. *Nat. Rev. Clin. Oncol.* **17**, 147–167 (2020). doi:10.1038/s41571-019-0297-y Medline

23. A. F. Labrijn, M. L. Janmaat, J. M. Reichert, P. W. H. I. Parren, Bispecific antibodies: A mechanistic review of the pipeline. *Nat. Rev. Drug Discov.* **18**, 585–608 (2019). doi:10.1038/s41573-019-0028-1 Medline

24. H. Kantarjian, A. Stein, N. Gökbuget, A. K. Fielding, A. C. Schuh, J.-M. Ribera, A. Wei, H. Dombret, R. Foà, R. Bassan, Ö. Arslan, M. A. Sanz, J. Bergeron, F. Demirkan, E. Lech-Maranda, A. Rambaldi, X. Thomas, H.-A. Horst, M. Brüggemann, W. Klapper, B. L. Wood, A. Fleishman, D. Nagorsen, C. Holland, Z. Zimmerman, M. S. Topp, Blinatumomab versus chemotherapy for advanced acute lymphoblastic leukemia. *N. Engl. J. Med.* **376**, 836–847 (2017). doi:10.1056/NEJMoa1609783 Medline

25. M. Andreatta, M. Nielsen, Gapped sequence alignment using artificial neural networks: Application to the MHC class I system. *Bioinformatics* **32**, 511–517 (2016). doi:10.1093/bioinformatics/btv639 Medline

26. M. R. Parkhurst, P. F. Robbins, E. Tran, T. D. Prickett, J. J. Gartner, L. Jia, G. Ivey, Y. F. Li, M. El-Gamil, A. Lalani, J. S. Crystal, A. Sachs, E. Groh, S. Ray, L. T. Ngo, S. Kivitz, A. Pasetto, R. Yossef, F. J. Lowery, S. L. Goff, W. Lo, G. Cafri, D. C. Deniger, P. Malekzadeh, M. Ahmadzadeh, J. R. Wunderlich, R. P. T. Somerville, S. A. Rosenberg, Unique neoantigens arise from somatic mutations in patients with gastrointestinal cancers. *Cancer Discov.* **9**, 1022–1035 (2019). doi:10.1158/2159-8290.CD-18-1494 Medline

27. Q. Wang, J. Douglass, M. S. Hwang, E. H. Hsiue, B. J. Mog, M. Zhang, N. Papadopoulos, K. W. Kinzler, S. Zhou, B. Vogelstein, Direct detection and quantification of neoantigens. *Cancer Immunol. Res.* **7**, 1748–1754 (2019). doi:10.1158/2326-6066.CIR-19-0107 Medline

28. M. S. Miller, J. Douglass, M. S. Hwang, A. D. Skora, M. Murphy, N. Papadopoulos, K. W. Kinzler, B. Vogelstein, S. Zhou, S. B. Gabelli, An engineered antibody fragment targeting mutant β-catenin via major histocompatibility complex I neoantigen presentation. *J. Biol. Chem.* **294**, 19322–19334 (2019). doi:10.1074/jbc.RA119.010251 Medline

29. J. Douglass, E. H.-C. Hsiue, B. J. Mog, M. S. Hwang, S. R. DiNapoli, A. H. Pearlman, M. S. Miller, K. M. Wright, P. A. Azurmendi, Q. Wang, S. Paul, A. Schaefer, A. D. Skora, M. Dal Molin, M. F. Konig, Q. Liu, E. Watson, Y. Li, M. B. Murphy, D. M. Pardoll, C. Bettegowda, N. Papadopoulos, S. B. Gabelli, K. W. Kinzler, B. Vogelstein, S. Zhou, Bispecific antibodies targeting mutant, neoantigens. *Sci. Immunol.* **6**, eabd5515 (2021).

30. S. Paul, A. H. Pearlman, J. Douglass, B. J. Mog, E. H.-C. Hsiue, M. S. Hwang, S. R. DiNapoli, M. F. Konig, P. A. Brown, K. M. Wright, S. Sur, S. B. Gabelli, Y. Li, G. Ghiaur, D. Pardoll, N. Papadopoulos, C. Bettegowda, K. W. Kinzler, S. Zhou, B. Vogelstein, TCR beta chain-directed bispecific antibodies for the treatment of T cell cancers. *Sci. Transl. Med.* 10.1126/scitranslmed.abd3595 (2021).

31. H. Wu, D. G. Myszka, S. W. Tendian, C. G. Brouillette, R. W. Sweet, I. M. Chaiken, W. A. Hendrickson, Kinetic and structural analysis of mutant CD4 receptors that are defective in HIV gp120 binding. *Proc. Natl. Acad. Sci. U.S.A.* **93**, 15030–15035 (1996). doi:10.1073/pnas.93.26.15030 Medline

32. P. C. Beverley, R. E. Callard, Distinctive functional characteristics of human “T” lymphocytes defined by E rosetting or a monoclonal anti-T cell antibody. *Eur. J. Immunol.* **11**, 329–334 (1981). doi:10.1002/eji.1830110412 Medline

33. Z. Zhu, G. D. Lewis, P. Carter, Engineering high affinity humanized anti-p185HER2/anti-CD3 bispecific F(ab’)2 for efficient lysis of p185HER2 overexpressing tumor cells. *Int. J. Cancer* **62**, 319–324 (1995). doi:10.1002/ijc.2910620315 Medline

34. T. Dreier, G. Lorenczewski, C. Brandl, P. Hoffmann, U. Syring, F. Hanakam, P. Kufer, G. Riethmuller, R. Bargou, P. A. Baeuerle, Extremely potent, rapid and costimulation-independent cytotoxic T-cell response against lymphoma cells catalyzed by a single-chain bispecific antibody. *Int. J. Cancer* **100**, 690–697 (2002). doi:10.1002/ijc.10557 Medline

35. J. P. Van Wauwe, J. R. De Mey, J. G. Goossens, OKT3: A monoclonal anti-human T lymphocyte antibody with potent mitogenic properties. *J. Immunol.* **124**, 2708–2713 (1980). Medline

36. L. Huang, L. S. Johnson, CD3-binding molecules capable of binding to human and non-human CD3. Macrogenics (2014).

37. E. Krissinel, K. Henrick, Inference of macromolecular assemblies from crystalline state. *J. Mol. Biol.* **372**, 774–797 (2007). doi:10.1016/j.jmb.2007.05.022 Medline

38. S. Sarkizova, S. Klaeger, P. M. Le, L. W. Li, G. Oliveira, H. Keshishian, C. R. Hartigan, W. Zhang, D. A. Braun, K. L. Ligon, P. Bachireddy, I. K. Zervantonakis, J. M. Rosenbluth, T. Ouspenskaia, T. Law, S. Justesen, J. Stevens, W. J. Lane, T. Eisenhaure, G. Lan Zhang, K. R. Clauser, N. Hacohen, S. A. Carr, C. J. Wu, D. B. Keskin, A large peptidome dataset improves HLA class I epitope prediction across most of the human population. *Nat. Biotechnol.* **38**, 199–209 (2020). doi:10.1038/s41587-019-0322-9 Medline

39. A. I. Webb, M. A. Dunstone, W. Chen, M. I. Aguilar, Q. Chen, H. Jackson, L. Chang, L. Kjer-Nielsen, T. Beddoe, J. McCluskey, J. Rossjohn, A. W. Purcell, Functional and structural characteristics of NY-ESO-1-related HLA A2-restricted epitopes and the design of a novel immunogenic analogue. *J. Biol. Chem.* **279**, 23438–23446 (2004). doi:10.1074/jbc.M314066200 Medline

40. N. Ataie, J. Xiang, N. Cheng, E. J. Brea, W. Lu, D. A. Scheinberg, C. Liu, H. L. Ng, Structure of a TCR-mimic antibody with target predicts pharmacogenetics. *J. Mol. Biol.* **428**, 194–205 (2016). doi:10.1016/j.jmb.2015.12.002 Medline

41. R. S. Gejman, H. F. Jones, M. G. Klatt, A. Y. Chang, C. Y. Oh, S. S. Chandran, T. Korontsvit, V. Zakahleva, T. Dao, C. A. Klebanoff, D. A. Scheinberg, Identification of the targets of T-cell receptor therapeutic agents and cells by use of a high-throughput genetic platform. *Cancer Immunol. Res.* **8**, 672–684 (2020). doi:10.1158/2326-6066.CIR-19-0745 Medline

42. T. Kula, M. H. Dezfulian, C. I. Wang, N. S. Abdelfattah, Z. C. Hartman, K. W. Wucherpfennig, H. K. Lyerly, S. J. Elledge, T-Scan: A genome-wide method for the systematic discovery of T cell epitopes. *Cell* **178**, 1016–1028.e13 (2019). doi:10.1016/j.cell.2019.07.009 Medline

43. C. H. Coles, R. M. Mulvaney, S. Malla, A. Walker, K. J. Smith, A. Lloyd, K. L. Lowe, M. L. McCully, R. Martinez Hague, M. Aleksic, J. Harper, S. J. Paston, Z. Donnellan, F. Chester, K. Wiederhold, R. A. Robinson, A. Knox, A. R. Stacey, J. Dukes, E. Baston, S. Griffin, B. K. Jakobsen, A. Vuidepot, S. Harper, TCRs with distinct specificity profiles use different binding modes to engage an identical peptide-HLA complex. *J. Immunol.* **204**, 1943–1953 (2020). doi:10.4049/jimmunol.1900915 Medline

44. J. Harper, K. J. Adams, G. Bossi, D. E. Wright, A. R. Stacey, N. Bedke, R. Martinez-Hague, D. Blat, L. Humbert, H. Buchanan, G. S. Le Provost, Z. Donnellan, R. J. Carreira, S. J. Paston, L. U. Weigand, M. Canestraro, J. P. Sanderson, S. Botta Gordon-Smith, K. L. Lowe, K. A. Rygiel, A. S. Powlesland, A. Vuidepot, N. J. Hassan, B. J. Cameron, B. K. Jakobsen, J. Dukes, An approved in vitro approach to preclinical safety and efficacy evaluation of engineered T cell receptor anti-CD3 bispecific (ImmTAC) molecules. *PLOS ONE* **13**, e0205491 (2018). doi:10.1371/journal.pone.0205491 Medline

45. E. de Castro, C. J. Sigrist, A. Gattiker, V. Bulliard, P. S. Langendijk-Genevaux, E. Gasteiger, A. Bairoch, N. Hulo, ScanProsite: Detection of PROSITE signature matches and ProRule-associated functional and structural residues in proteins. *Nucleic Acids Res.* **34**, W362-5 (2006). doi:10.1093/nar/gkl124 Medline

46. G. Stewart-Jones, A. Wadle, A. Hombach, E. Shenderov, G. Held, E. Fischer, S. Kleber, N. Nuber, F. Stenner-Liewen, S. Bauer, A. McMichael, A. Knuth, H. Abken, A. A. Hombach, V. Cerundolo, E. Y. Jones, C. Renner, Rational development of high-affinity

T-cell receptor-like antibodies. *Proc. Natl. Acad. Sci. U.S.A.* **106**, 5784–5788 (2009). doi:10.1073/pnas.0901425106 Medline

47. M. C. Raman, P. J. Rizkallah, R. Simmons, Z. Donnellan, J. Dukes, G. Bossi, G. S. Le Provost, P. Todorov, E. Baston, E. Hickman, T. Mahon, N. Hassan, A. Vuidepot, M. Sami, D. K. Cole, B. K. Jakobsen, Direct molecular mimicry enables off-target cardiovascular toxicity by an enhanced affinity TCR designed for cancer immunotherapy. *Sci. Rep.* **6**, 18851 (2016). doi:10.1038/srep18851 Medline

48. N. Liddy, G. Bossi, K. J. Adams, A. Lissina, T. M. Mahon, N. J. Hassan, J. Gavarret, F. C. Bianchi, N. J. Pumphrey, K. Ladell, E. Gostick, A. K. Sewell, N. M. Lissin, N. E. Harwood, P. E. Molloy, Y. Li, B. J. Cameron, M. Sami, E. E. Baston, P. T. Todorov, S. J. Paston, R. E. Dennis, J. V. Harper, S. M. Dunn, R. Ashfield, A. Johnson, Y. McGrath, G. Plesa, C. H. June, M. Kalos, D. A. Price, A. Vuidepot, D. D. Williams, D. H. Sutton, B. K. Jakobsen, Monoclonal TCR-redirected tumor cell killing. *Nat. Med.* **18**, 980–987 (2012). doi:10.1038/nm.2764 Medline

49. M. A. Purbhoo, D. J. Irvine, J. B. Huppa, M. M. Davis, T cell killing does not require the formation of a stable mature immunological synapse. *Nat. Immunol.* **5**, 524–530 (2004). doi:10.1038/ni1058 Medline

50. J. D. Stone, D. H. Aggen, A. Schietinger, H. Schreiber, D. M. Kranz, A sensitivity scale for targeting T cells with chimeric antigen receptors (CARs) and bispecific T-cell Engagers (BiTEs). *OncoImmunology* **1**, 863–873 (2012). doi:10.4161/onci.20592 Medline

51. G. P. Dunn, C. M. Koebel, R. D. Schreiber, Interferons, immunity and cancer immunoediting. *Nat. Rev. Immunol.* **6**, 836–848 (2006). doi:10.1038/nri1961 Medline

52. B. J. Cameron, A. B. Gerry, J. Dukes, J. V. Harper, V. Kannan, F. C. Bianchi, F. Grand, J. E. Brewer, M. Gupta, G. Plesa, G. Bossi, A. Vuidepot, A. S. Powlesland, A. Legg, K. J. Adams, A. D. Bennett, N. J. Pumphrey, D. D. Williams, G. Binder-Scholl, I. Kulikovskaya, B. L. Levine, J. L. Riley, A. Varela-Rohena, E. A. Stadtmauer, A. P. Rapoport, G. P. Linette, C. H. June, N. J. Hassan, M. Kalos, B. K. Jakobsen, Identification of a Titin-derived HLA-A1-presented peptide as a cross-reactive target for engineered MAGE A3-directed T cells. *Sci. Transl. Med.* **5**, 197ra103 (2013). doi:10.1126/scitranslmed.3006034 Medline

53. R. A. Morgan, N. Chinnasamy, D. Abate-Daga, A. Gros, P. F. Robbins, Z. Zheng, M. E. Dudley, S. A. Feldman, J. C. Yang, R. M. Sherry, G. Q. Phan, M. S. Hughes, U. S. Kammula, A. D. Miller, C. J. Hessman, A. A. Stewart, N. P. Restifo, M. M. Quezado, M. Alimchandani, A. Z. Rosenberg, A. Nath, T. Wang, B. Bielekova, S. C. Wuest, N. Akula, F. J. McMahon, S. Wilde, B. Mosetter, D. J. Schendel, C. M. Laurencot, S. A. Rosenberg, Cancer regression and neurological toxicity following anti-MAGE-A3 TCR gene therapy. *J. Immunother.* **36**, 133–151 (2013). doi:10.1097/CJI.0b013e3182829903 Medline

54. A. G. Chapuis, D. N. Egan, M. Bar, T. M. Schmitt, M. S. McAfee, K. G. Paulson, V. Voillet, R. Gottardo, G. B. Ragnarsson, M. Bleakley, C. C. Yeung, P. Muhlhauser, H. N. Nguyen, L. A. Kropp, L. Castelli, F. Wagener, D. Hunter, M. Lindberg, K. Cohen, A. Seese, M. J. McElrath, N. Duerkopp, T. A. Gooley, P. D. Greenberg, T cell receptor gene therapy

targeting WT1 prevents acute myeloid leukemia relapse post-transplant. *Nat. Med.* **25**, 1064–1072 (2019). doi:10.1038/s41591-019-0472-9 Medline

55. E. Tran, P. F. Robbins, Y. C. Lu, T. D. Prickett, J. J. Gartner, L. Jia, A. Pasetto, Z. Zheng, S. Ray, E. M. Groh, I. R. Kriley, S. A. Rosenberg, T-cell transfer therapy targeting mutant KRAS in cancer. *N. Engl. J. Med.* **375**, 2255–2262 (2016). doi:10.1056/NEJMoa1609279 Medline

56. M. E. Goebeler, R. C. Bargou, T cell-engaging therapies - BiTEs and beyond. *Nat. Rev. Clin. Oncol.* **17**, 418–434 (2020). doi:10.1038/s41571-020-0347-5 Medline

57. W. A. Jefferies, G. G. MacPherson, Expression of the W6/32 HLA epitope by cells of rat, mouse, human and other species: Critical dependence on the interaction of specific MHC heavy chains with human or bovine beta 2-microglobulin. *Eur. J. Immunol.* **17**, 1257–1263 (1987). doi:10.1002/eji.1830170907 Medline

58. A. D. Skora, J. Douglass, M. S. Hwang, A. J. Tam, R. L. Blosser, S. B. Gabelli, J. Cao, L. A. Diaz Jr., N. Papadopoulos, K. W. Kinzler, B. Vogelstein, S. Zhou, Generation of MANAbodies specific to HLA-restricted epitopes encoded by somatically mutated genes. *Proc. Natl. Acad. Sci. U.S.A.* **112**, 9967–9972 (2015). doi:10.1073/pnas.1511996112 Medline

59. Y. Huang, B. Niu, Y. Gao, L. Fu, W. Li, CD-HIT Suite: A web server for clustering and comparing biological sequences. *Bioinformatics* **26**, 680–682 (2010). doi:10.1093/bioinformatics/btq003 Medline

60. D. G. Myszka, Improving biosensor analysis. *J. Mol. Recognit.* **12**, 279–284 (1999). doi:10.1002/(SICI)1099-1352(199909/10)12:5<279:AID-JMR473>3.0.CO;2-3 Medline

61. F. H. Niesen, H. Berglund, M. Vedadi, The use of differential scanning fluorimetry to detect ligand interactions that promote protein stability. *Nat. Protoc.* **2**, 2212–2221 (2007). doi:10.1038/nprot.2007.321 Medline

62. U. B. Ericsson, B. M. Hallberg, G. T. Detitta, N. Dekker, P. Nordlund, Thermofluor-based high-throughput stability optimization of proteins for structural studies. *Anal. Biochem.* **357**, 289–298 (2006). doi:10.1016/j.ab.2006.07.027 Medline

63. M. Cheng, B. H. Santich, H. Xu, M. Ahmed, M. Huse, N. K. Cheung, Successful engineering of a highly potent single-chain variable-fragment (scFv) bispecific antibody to target disialoganglioside (GD2) positive tumors. *OncoImmunology* **5**, e1168557 (2016). doi:10.1080/2162402X.2016.1168557 Medline

64. J. D. Altman, M. M. Davis, MHC-peptide tetramers to visualize antigen-specific T cells. *Curr. Protoc. Immunol.* **115**, 17.13.11–17.13, 44 (2016). doi:10.1002/cpim.14 Medline

65. D. N. Garboczi, D. T. Hung, D. C. Wiley, HLA-A2-peptide complexes: Refolding and crystallization of molecules expressed in *Escherichia coli* and complexed with single antigenic peptides. *Proc. Natl. Acad. Sci. U.S.A.* **89**, 3429–3433 (1992). doi:10.1073/pnas.89.8.3429 Medline

66. F. W. Studier, Protein production by auto-induction in high density shaking cultures. *Protein Expr. Purif.* **41**, 207–234 (2005). doi:10.1016/j.pep.2005.01.016 Medline

67. G. Winter, K. E. McAuley, Automated data collection for macromolecular crystallography. *Methods* **55**, 81–93 (2011). doi:10.1016/j.ymeth.2011.06.010 Medline

68. W. Kabsch, Xds. *Acta Crystallogr. D Biol. Crystallogr.* **66**, 125–132 (2010). doi:10.1107/S0907444909047337 Medline

69. P. R. Evans, G. N. Murshudov, How good are my data and what is the resolution? *Acta Crystallogr. D Biol. Crystallogr.* **69**, 1204–1214 (2013). doi:10.1107/S0907444913000061 Medline

70. A. J. McCoy, R. W. Grosse-Kunstleve, P. D. Adams, M. D. Winn, L. C. Storoni, R. J. Read, *Phaser* crystallographic software. *J. Appl. Crystallogr.* **40**, 658–674 (2007). doi:10.1107/S0021889807021206 Medline

71. M. Mishto, A. Mansurkhodzhaev, G. Ying, A. Bitra, R. A. Cordfunke, S. Henze, D. Paul, J. Sidney, H. Urlaub, J. Neefjes, A. Sette, D. M. Zajonc, J. Liepe, An in silico–in vitro pipeline identifying an HLA-A*02:01^{+} KRAS G12V^{+} spliced epitope candidate for a broad tumor-immune response in cancer patients. *Front. Immunol.* **10**, 2572 (2019). doi:10.3389/fimmu.2019.02572 Medline

72. M. D. Winn, C. C. Ballard, K. D. Cowtan, E. J. Dodson, P. Emsley, P. R. Evans, R. M. Keegan, E. B. Krissinel, A. G. Leslie, A. McCoy, S. J. McNicholas, G. N. Murshudov, N. S. Pannu, E. A. Potterton, H. R. Powell, R. J. Read, A. Vagin, K. S. Wilson, Overview of the *CCP*4 suite and current developments. *Acta Crystallogr. D Biol. Crystallogr.* **67**, 235–242 (2011). doi:10.1107/S0907444910045749 Medline

73. G. N. Murshudov, A. A. Vagin, E. J. Dodson, Refinement of macromolecular structures by the maximum-likelihood method. *Acta Crystallogr. D Biol. Crystallogr.* **53**, 240–255 (1997). doi:10.1107/S0907444996012255 Medline

74. P. Emsley, B. Lohkamp, W. G. Scott, K. Cowtan, Features and development of Coot. *Acta Crystallogr. D Biol. Crystallogr.* **66**, 486–501 (2010). doi:10.1107/S0907444910007493 Medline

75. R. Gowthaman, B. G. Pierce, TCR3d: The T cell receptor structural repertoire database. *Bioinformatics* **35**, 5323–5325 (2019). doi:10.1093/bioinformatics/btz517 Medline

76. B. G. Pierce, Z. Weng, A flexible docking approach for prediction of T cell receptor-peptide-MHC complexes. *Protein Sci.* **22**, 35–46 (2013). doi:10.1002/pro.2181 Medline

77. N. Yoshiya, S. Adachi, Y. Misawa, H. Yuzawa, T. Honda, K. Kanazawa, K. Takeuchi S Tanaka, K. Tanaka, [Isolation of cisplatin-resistant subline from human ovarian cancer cell line and analysis of its cell-biological characteristics]. *Nippon Sanka Fujinka Gakkai Zasshi* **41**, 7–14 (1989). Medline

78. P. J. Miller, Y. Pazy, B. Conti, D. Riddle, E. Appella, E. J. Collins, Single MHC mutation eliminates enthalpy associated with T cell receptor binding. *J. Mol. Biol.* **373**, 315–327 (2007). doi:10.1016/j.jmb.2007.07.028 Medline

79. H. W. Nijman, J. G. Houbiers, M. P. Vierboom, S. H. van der Burg, J. W. Drijfhout, J. D'Amaro, P. Kenemans, C. J. Melief, W. M. Kast, Identification of peptide sequences that potentially trigger HLA-A2.1-restricted cytotoxic T lymphocytes. *Eur. J. Immunol.* **23**, 1215–1219 (1993). doi:10.1002/eji.1830230603 Medline

80. Q. Li, D. Hapka, H. Chen, D. A. Vallera, C. R. Wagner, Self-assembly of antibodies by chemical induction. *Angew. Chem. Int. Ed.* **47**, 10179–10182 (2008). doi:10.1002/anie.200803507 Medline

81. T. T. Junttila, J. Li, J. Johnston, M. Hristopoulos, R. Clark, D. Ellerman, B.-E. Wang, Y. Li, M. Mathieu, G. Li, J. Young, E. Luis, G. Lewis Phillips, E. Stefanich, C. Spiess, A. Polson, B. Irving, J. M. Scheer, M. R. Junttila, M. S. Dennis, R. Kelley, K. Totpal, A. Ebens, Antitumor efficacy of a bispecific antibody that targets HER2 and activates T cells. *Cancer Res.* **74**, 5561–5571 (2014). doi:10.1158/0008-5472.CAN-13-3622-T Medline

82. U. Reusch, J. Duell, K. Ellwanger, C. Herbrecht, S. H. J. Knackmuss, I. Fucek, M. Eser, F. McAleese, V. Molkenthin, F. L. Gall, M. Topp, M. Little, E. A. Zhukovsky, A tetravalent bispecific TandAb (CD19/CD3), AFM11, efficiently recruits T cells for the potent lysis of $CD19^+$ tumor cells. *MAbs* **7**, 584–604 (2015). doi:10.1080/19420862.2015.1029216 Medline

83. L. Kjer-Nielsen, M. A. Dunstone, L. Kostenko, L. K. Ely, T. Beddoe, N. A. Mifsud, A. W. Purcell, A. G. Brooks, J. McCluskey, J. Rossjohn, Crystal structure of the human T cell receptor CD3 epsilon gamma heterodimer complexed to the therapeutic mAb OKT3. *Proc. Natl. Acad. Sci. U.S.A.* **101**, 7675–7680 (2004). doi:10.1073/pnas.0402295101 Medline

84. L. Liu, C. K. Lam, V. Long, L. Widjaja, Y. Yang, H. Li, L. Jin, S. Burke, S. Gorlatov, J. Brown, R. Alderson, M. D. Lewis, J. L. Nordstrom, S. Koenig, P. A. Moore, S. Johnson, E. Bonvini, MGD011, A CD19 x CD3 dual-affinity retargeting bi-specific molecule incorporating extended circulating half-life for the treatment of B-cell malignancies. *Clin. Cancer Res.* **23**, 1506–1518 (2017). doi:10.1158/1078-0432.CCR-16-0666 Medline